

Electrical and Mechanical Properties of Poly(L-lactide)/Carbon Nanotubes/Clay Nanocomposites

Hun-Sik Kim, Ha Il Kwon, Soon-Min Kwon, Young Soo Yun, Jin-San Yoon, and Hyoung-Joon Jin*

Department of Polymer Science and Engineering, Inha University, 402-751 Incheon, Korea

An organoclay containing epoxy groups, twice-functionalized organoclay (TFC), was synthesized by reacting (glycidoxypropyl)trimethoxy silane with Cloisite25A® (C25A), which had already been modified with an amine compound. The introduction of epoxy groups to the clay surface and carboxylic group-functionalized multiwalled carbon nanotubes (MWCNTs) improved the interfacial adhesion between the poly(L-lactide) (PLLA) and nano-sized fillers when melt-compounded. The PLLA/MWCNTs/TFC nanocomposites showed superior tensile properties to those of PLLA and PLLA/CNTs. The dispersion of MWCNTs in the PLLA matrix decreased the electrical resistivity of the composite substantially due to the higher MWCNT loading. However, the introduction of TFC to the PLLA/MWCNTs nanocomposites resulted in a slight increase in volume resistivity. This increase was attributed to the individual MWCNTs being blocked by the TFC. The clays in the PLLA/MWCNTs/TFC nanocomposites prevented direct contact between the neighboring MWCNTs, which increased the electrical resistivity of the nanocomposites.

Keywords: Carbon Nanotube, Clay, Poly(L-lactide), Electrical Conductivity, Mechanical Properties, Nanocomposite.

IP: 127.0.0.1 On: Fri, 22 May 2020 02:15:39
Copyright: American Scientific Publishers
Delivered by Ingenta

1. INTRODUCTION

Carbon nanotubes (CNTs) and clay are two of the most promising candidates for the design of novel, ultrahigh strength polymer composites.^{1–3} However, these novel, ultrahigh strength polymer composites require a uniform dispersion of the CNTs and/or clay in a polymer matrix without aggregation. In addition, they require a strong interaction between the nano-sized fillers and polymer matrix.⁴ Thus far, the potential benefits of nanocomposites have not been fully realized due to the difficulties involved in their preparation. In addition, good interfacial adhesion is important for efficient load transfer in the composite.⁵ Both noncovalent and covalent modifications of the nano-sized filler surface have been used to improve the surface wettability and solubility.⁶

Poly(L-lactide) (PLLA) is currently used widely in architecture, automobiles, biomedicine and single-use products.^{7,8} However, the relatively high price of PLLA precludes its more general application. Therefore, many attempts have been made to give PLLA multifunctional properties.

Several studies have examined PLLA based nanocomposites prepared by *in situ* polymerization,⁹ solution mixing¹⁰ and melt blending.¹¹ Chen et al.¹² reported that the mechanical behavior of PLLA/twice functionalized organoclay (TFC) was increased significantly by the incorporation of TFC. Clay is a potential reinforcing agent for PLLA on account of its superior mechanical properties and high aspect ratio. Chen et al.¹³ and Kim et al.¹⁴ reported that the mechanical behavior of PLLA/multiwalled carbon nanotubes (MWCNTs) was increased significantly by the incorporation of MWCNTs. However, there are few reports on the complex activity of the two types of nanofillers in a polymer matrix, when the two different nanofillers are incorporated at the same time. This study examined the properties of PLLA/MWCNTs and PLLA/MWCNTs/TFC nanocomposites.

2. EXPERIMENTAL DETAILS

PLLA was manufactured by Shimadzu Co., Japan with a weight average molecular weight of 1.6×10^5 g/mol. The as received MWCNTs (Ijin Nanotech Co., Korea), which were synthesized by chemical vapor deposition (CVD), had a carbon content of approximately 95%. The MWCNTs were treated with a mixture of 3 M HNO₃ and

*Author to whom correspondence should be addressed.

1 M H₂SO₄ at 60 °C for 12 h. These acid-treatments are known to introduce carboxylic functional groups to the surface of the MWCNTs.¹⁵ The organically modified clay (organoclay), Cloisite 25A® (C25A), was purchased from Southern Clay Product Inc., USA, and purified by suspension in ethanol at 70 °C for 4 h to remove contamination. The silane coupling agent, (glycidoxypopyl)trimethoxy silane (GPS), was supplied by Aldrich. The GPS was hydrolyzed with hydrochloric acid in an ethanol/deionized water (9:1 wt%) mixture at pH 4.0 for 4 h. C25A was then added and the resulting mixture was heated under reflux for 24 h hours at 70 °C. The product was dried in a vacuum oven for 48 h at 50 °C.¹⁶

To prepare the PLLA/MWCNTs nanocomposites, the resulting functionalized MWCNTs were allowed to swell in 600 ml of CHCl₃. The swollen functionalized MWCNTs were then sonicated in a bath (28 kHz) for 30 min. Subsequently, 40.0 g of PLLA was added followed by sonication for a further 30 min. The mixture was then dried in a convection oven for 24 h at room temperature. The following procedure was used to prepare the PLLA/MWCNTs/TFC nanocomposites. The swollen MWCNTs and TFC were sonicated in a bath for 30 min. Forty grams of PLLA was then added and the resulting mixture was sonicated for a further 30 min. The PLLA/MWCNTs/TFC batch was dried in a convection oven for 24 h at room temperature. The PLLA/MWCNTs and PLLA/MWCNTs/TFC nanocomposites were melt processed using a Brabender mixer at 180 °C for 30 min. The prepared nanocomposites were annealed at 60 °C for 12 h before characterization.

The tensile properties were tested on an Instron 4665 universal testing machine (UTM) at 20 °C and 30% humidity. The electrical properties of the nanocomposites were determined by measuring the volume resistivity (Ω · cm), which corresponds to the resistance, which is expressed as the unit volume. The morphology of the PLLA/MWCNTs and PLLA/MWCNTs/TFC nanocomposites were observed by scanning electron microscopy (SEM, Hitachi S-4300, Japan) at an accelerating voltage of 15 kV. The transmission electron microscopy (TEM) images were obtained using a JEM-2100F instrument (JEOL, Japan)

operating at an accelerating voltage of 100 kV. The glass transition temperatures (T_g), melting temperatures (T_m), heat of fusion at the melting process (ΔH_m) and crystallization temperature (T_c) of the PLLA/MWCNTs/TFC nanocomposites were measured using a differential scanning calorimeter (DSC, Perkin-Elmer DSC 7).

3. RESULTS AND DISCUSSION

Table I shows the tensile properties of the PLLA/MWCNTs and PLLA/MWCNTs/TFC nanocomposites. The number after the abbreviation is the weight percentage of MWCNTs and TFC in the nanocomposites. For example, PLLA/MWCNTs10/TFC10 is a composite composed of 1.0 wt% MWCNTs and 1.0 wt% TFC. The improved tensile properties were attributed the well dispersed MWCNTs and TFC in the polymer matrix.

According to Table I, the addition of the MWCNTs to PLLA increased the tensile modulus and strength, which suggests that the MWCNTs acted as a reinforcing filler due to their high aspect ratio and tensile properties. In addition, the tensile modulus was increased by the addition of TFC to the PLLA/MWCNTs nanocomposites on account of its high tensile properties and platelet structure. However, the elongation at break of the PLLA/MWCNTs and PLLA/MWCNTs/TFC nanocomposites decreased with increasing MWCNTs and TFC content.

SEM was used to analyze the morphological evolution of the PLLA/MWCNTs and PLLA/MWCNTs/TFC nanocomposites. Figure 1 shows SEM images of the fractured surface of the PLLA/MWCNTs and PLLA/MWCNTs/TFC nanocomposites.

Figure 1(a) shows a substantial amount of MWCNTs well dispersed in the PLLA matrix of the PLLA/MWCNTs10 nanocomposite. TFC was also well dispersed in the PLLA/MWCNTs/TFC matrix, as shown in Figure 1(b). The clay had the appearance of a flake or leaf-shaped unit. Some of the individual particles were approximately 0.5~2 μm thick. Therefore, at least some clay breaks down relatively easily into flakes approaching the unit-cell thickness.¹⁷ Each flake-shaped silicate particle

Table I. The tensile properties of PLLA, PLLA/MWCNTs, and PLLA/MWCNTs/TFC nanocomposites.

Samples	MWCNT (wt%)	TFC (wt%)	Tensile strength (MPa)	Young's modulus (GPa)	Elongation at break (%)
PLLA	—	—	48.2 ± 2.7	2.1 ± 0.3	6.4 ± 0.9
PLLA/MWCNTs05	0.5	—	49.5 ± 1.9	2.5 ± 0.4	6.1 ± 1.2
PLLA/MWCNTs05/TFC05	0.5	0.5	56.6 ± 1.1	2.7 ± 0.5	5.8 ± 1.3
PLLA/MWCNTs05/TFC10	0.5	1.0	61.1 ± 0.8	3.2 ± 0.5	5.7 ± 0.8
PLLA/MWCNTs05/TFC20	0.5	2.0	65.4 ± 0.6	3.8 ± 0.6	5.5 ± 0.7
PLLA/MWCNTs10	1.0	—	55.3 ± 0.8	2.6 ± 0.5	5.8 ± 0.9
PLLA/MWCNTs10/TFC05	1.0	0.5	60.4 ± 0.8	2.6 ± 0.3	5.7 ± 1.0
PLLA/MWCNTs10/TFC10	1.0	1.0	63.1 ± 0.6	3.4 ± 0.5	5.8 ± 0.9
PLLA/MWCNTs10/TFC20	1.0	2.0	70.4 ± 0.5	4.0 ± 0.6	4.7 ± 0.7
PLLA/MWCNTs20	2.0	—	61.5 ± 0.8	2.9 ± 0.3	5.5 ± 1.1

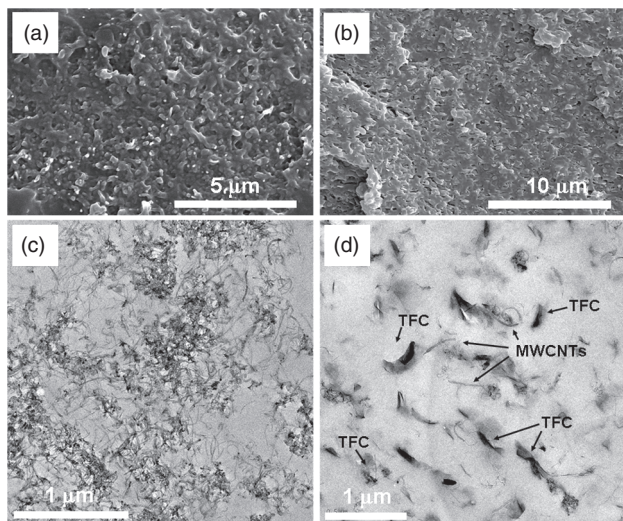


Fig. 1. SEM and TEM images of (a, c) PLLA/MWCNTs10, and (b, d) PLLA/MWCNTs10/TFC20 nanocomposites.

contained stacked layers, tactoids, with an interlayer distance of approximately 18 Å according to XRD (comments in Fig. 3).¹²

The electrical resistivity of the PLLA/MWCNTs nanocomposites decreased rapidly with increasing MWCNT loading (1.8×10^{15} (0 wt%) to $6.6 \times 10^3 \Omega \cdot \text{cm}$ (2.0 wt%)).¹⁴ The following conduction mechanism of the polymer/CNTs composites is proposed. The filler makes a three dimensional conducting network in the matrix when a highly conducting filler, such as CNTs or carbon black (CB), is incorporated into the polymer matrix.^{18,19}

Figure 2 shows that the electrical resistivity of the PLLA/MWCNTs/TFC nanocomposites increases with increasing TFC content. In the case of PLLA/MWCNTs10, the electrical resistivity increased from $6.8 \times 10^7 \Omega \cdot \text{cm}$ to $8.6 \times 10^{13} \Omega \cdot \text{cm}$ when 2.0 wt% TFC was added. In addition, the electrical resistivity of PLLA/MWCNTs05/TFC20 was higher than PLLA/MWCNTs05 (from 3.6×10^{13} to $9.6 \times 10^{15} \Omega \cdot \text{cm}$). This was attributed to the insulating property of TFC. The MWCNTs in the

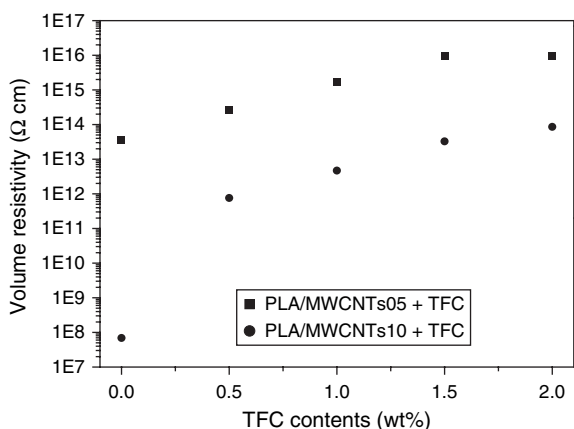


Fig. 2. Electrical properties of PLLA/MWCNTs/TFC nanocomposites.

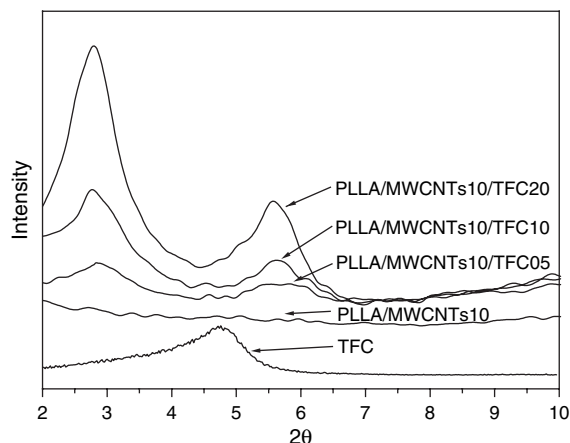


Fig. 3. X-ray diffraction patterns of PLLA/MWCNTs10/TFC nanocomposites.

PLLA/MWCNTs/TFC produce an electrically connected network that is hindered by TFC. This can explain the relatively low electrical conductivity of the PLLA/MWCNTs/TFC nanocomposites, even though the MWCNT loading was high enough to connect the MWCNTs to each other to form a network in a polymer matrix.

Figure 3 shows the XRD patterns of TFC and PLLA/MWCNTs/TFC. Intercalation of the polymer chains would increase the interlayer spacing compared to that of TFC, which would shift the XRD peak towards a lower angle. In the case of nanocomposites containing 2.0 wt% of the respective clays, the d spacing between the layers expanded from 18.4 to 32.0 and 31.6 Å for PLLA/MWCNTs05/TFC20 and PLLA/MWCNTs10/TFC20, respectively. The intensity of the $d(001)$ peak decreased with decreasing TFC content in the PLLA/MWCNTs/TFC nanocomposite and shifted slightly toward a lower diffraction angle. For example, for PLLA/MWCNTs10/TFC20, the 2θ angle was 2.79° (31.6 Å), while the 2θ angle for PLLA/MWCNTs10/TFC10 and PLLA/MWCNTs10/TFC05 was 2.76 and 2.69° (32.0 and 32.8 Å), respectively. The same trend was observed for the PLLA/MWCNTs05/TFC nanocomposites (data not shown).

The small peak at 5.7° was assigned to the $d(002)$ plane of the clay. The increase in d spacing of the nanocomposites compared to that of the corresponding neat TFC suggests that the PLLA molecules were inserted into the interlayer of the TFC.

The intercalation/exfoliation coexistence in the PLLA/MWCNTs/TFC nanocomposite was confirmed by TEM. Figures 1(c and d) shows a typical TEM image of the PLLA/MWCNTs10/TFC nanocomposites. Figure 1(c) shows the MWCNTs well dispersed in the polymer matrix. Therefore, the stacks of MWCNTs and TFC are well dispersed in the PLLA matrix, as shown in Figure 1(d).¹²

Table II. The thermal properties of PLLA, PLLA/MWCNTs, and PLLA/MWCNTs/TFC nanocomposites.

Samples	T_g (°C)	T_m (°C)	ΔH_m (J/g)	T_c (°C)
PLLA	51.5	167.4	12.9	94.5
PLLA/MWCNTs05	51.9	167.7	40.3	100.5
PLLA/MWCNTs05/TFC05	55.5	168.6	44.5	100.9
PLLA/MWCNTs05/TFC10	56.9	169.1	43.8	102.9
PLLA/MWCNTs05/TFC20	57.0	169.1	43.0	103.9
PLLA/MWCNTs10	52.5	167.6	42.1	104.6
PLLA/MWCNTs10/TFC05	56.4	168.4	49.2	106.2
PLLA/MWCNTs10/TFC10	57.1	168.1	48.2	107.6
PLLA/MWCNTs10/TFC20	57.3	168.1	45.5	109.8
PLLA/MWCNTs20	52.9	167.8	43.4	105.6

Table II shows the thermal properties of the PLLA/MWCNTs and PLLA/MWCNTs/TFC nanocomposites. The T_g of the polymer matrix depends on the free volume of the polymer, which is related to the affinity between the filler and polymer matrix. The SEM and TEM showed that the acid treated MWCNTs have good affinity toward the PLLA matrix, increasing the free volume beyond that of neat PLLA. Acid-modified MWCNTs may form hydrogen bonds with the ester groups of the PLLA molecules. In addition, the epoxy groups of TFC may react with the carboxyl groups of PLLA. The covalent bonding between TFC and PLLA was stronger than the hydrogen bonding between MWCNTs and PLLA. Therefore, a covalent bond results in a higher T_g of PLLA/MWCNTs/TFC than that produced by a hydrogen bond. The PLLA matrix showed a T_g of 51.5 °C. The T_g increased slightly when 0.5 wt% acid-treated MWCNTs were added to the matrix. The T_g of PLLA/MWCNTs05 was 51.9 °C, which is lower than that observed at an acid-treated MWCNTs content of 2.0 wt% (52.9 °C). The affinity between the acid treated MWCNTs and PLLA was quite good. Therefore, T_g decreases with increasing free volume of the composites. Moreover, TFC and MWCNTs increases the T_g of the PLLA nanocomposites. This is because TFC can form chemical bonds between the PLLA and epoxy group of TFC and/or carboxylic acid groups of the MWCNTs. These chemical interactions reduce the motion of the polymer chains. There were no significant changes in the melting temperature as the MWCNT content was increased.

In contrast, for TFC, the T_m increased slightly with increasing TFC content. The ΔH_m of pure PLLA was 12.9 J/g. In particular, the ΔH_m and T_c for all PLLA/MWCNTs and PLLA/MWCNTs/TFC nanocomposites were higher than that of pure PLLA. This higher ΔH_m , and T_c of the nanocomposites suggests higher crystallinity and easier crystallite formation. The increase in crystallinity was probably caused by the easy arrangement of the polymer chains due to the nucleating effect of MWCNTs and/or TFC in the nanocomposites.²⁰

4. CONCLUSION

The incorporation of a small amount of MWCNTs (0.5 and 1.0 wt%) improved the mechanical and electrical properties of the PLLA composites. The volume resistivity of the PLLA/MWCNTs nanocomposite showed an abrupt decrease (almost nine orders of magnitude) with 1.0 wt% MWCNTs. However, the electrical resistivity of the PLLA/MWCNTs nanocomposites increased with increasing TFC content. This was attributed to the insulating properties of TFC. Direct contact between the MWCNTs was impeded by the presence of TFC in the PLLA/MWCNTs/TFC nanocomposites. The intercalation of the polymer chains would increase the interlayer spacing compared to that of TFC, which would shift the XRD peak toward a lower angle. In the case of the PLLA/MWCNTs05/TFC20 and PLLA/MWCNTs10/TFC20, the d spacing between the layers increased from 18.4 to 32.0 and 31.6 Å, respectively. In the thermal study, the glass transition temperature was increased in the order: PLLA < PLLA/MWCNTs < PLLA/MWCNTs/TFC nanocomposites. This suggests that the incorporation of MWCNTs and TFC increased the glass transition temperature of the PLLA matrix, possibly due to chemical bonding between the PLLA molecules and carboxylic acid groups of MWCNTs and/or the epoxy group of TFC reducing the molecular motion of PLLA.

Acknowledgment: This work was supported by a grant (Code # 200810FTH010102001) from BioGreen21 Program, Rural Development Administration, Republic of Korea.

References and Notes

1. M. S. P. Shaffer and A. H. Windle, *Adv. Mater.* 11, 937 (1999).
2. S. Ijima, *Nature* 354, 56 (1991).
3. X.-L. Xie, Y.-W. Mai, and X.-P. Zhou, *Mater. Sci. Eng. R Rep.* 49, 89 (2005).
4. S.-M. Yuen, C.-C. M. Ma, Y.-Y. Lin, and H.-C. Kuan, *Compos. Sci. Technol.* 67, 2564 (2007).
5. X. Li, H. Gao, W. A. Scrivens, D. Fei, X. Xu, M. A. Sutton, A. P. Reynolds, P. Anthony, and M. L. Myrick, *J. Nanosci. Nanotechnol.* 7, 2309 (2007).
6. K. Fu and Y.-P. Sun, *J. Nanosci. Nanotechnol.* 3, 351 (2003).
7. S. Singh and S. S. Ray, *J. Nanosci. Nanotechnol.* 7, 2596 (2007).
8. M. Liu, J. Dong, Y. Yang, X. Yang, and H. Xu *J. Nanosci. Nanotechnol.* 8, 3493 (2008).
9. W. Song, Z. Zheng, W. Tang, and X. Wang, *Polymer* 48, 3658 (2007).
10. W.-M. Chiu, Y.-A. Chang, H.-Y. Kuo, M.-H. Lin, and H.-C. Wen, *J. Appl. Polym. Sci.* 108, 3024 (2008).
11. H.-S. Kim, B. H. Park, J. H. Choi, and J.-S. Yoon, *J. Appl. Polym. Sci.* 109, 3087 (2008).
12. G. X. Chen, H.-S. Kim, J. H. Shim, and J.-S. Yoon, *Macromolecules* 38, 3738 (2005).
13. G. X. Chen, H.-S. Kim, B. H. Park, and J.-S. Yoon, *Macromol. Chem. Phys.* 208, 389 (2007).
14. H.-S. Kim, B. H. Park, J.-S. Yoon, and H.-J. Jin, *Eur. Polym. J.* 43, 1729 (2007).

15. H.-S. Kim, W.-I. Park, M. Kang, and H.-J. Jin, *J. Phys. Chem. Solids* 69, 1209 (2008).
16. G. X. Chen and J.-S. Yoon, *Macromol. Rapid Commun.* 26, 899 (2005).
17. T. J. Pinnavaia and G. W. Beall, *Polymer-Clay Nanocomposites*, Wiley, New York (2005).
18. J. Sandler, M. S. P. Shaffer, T. Prasse, W. Bauhofer, K. Schulte, and A. H. Windle, *Polymer* 40, 5967 (1999).
19. Y. S. Song and J. R. Youn, *Carbon* 43, 1378 (2005).
20. E. Assouline, A. Lustiger, A. H. Barber, C. A. Cooper, E. Klein, E. Wachtel, and H. D. Wagner, *J. Polym. Sci. Pt. B-Polym. Phys.* 41, 520 (2003).

Received: 1 January 2009. Accepted: 1 July 2009.

IP: 127.0.0.1 On: Fri, 22 May 2020 02:15:39
Copyright: American Scientific Publishers
Delivered by Ingenta